Highly efficient CdS/CdTe solar cells investigated by cathodoluminescence spectroscopy

U. Jahn[*], *T. Okamoto*[**], *A. Yamada*[**]*, and M. Konagai*[**]

[*] Paul-Drude-Institut für Festkörperelektronik, Hausvogteiplatz 5-7, 10117 Berlin, Germany
[**] Department of Physical Electronics, Tokyo Institute of Technology, 2-12-1 O-okayama, Meguro-ku, Tokyo 152-8552, Japan

Abstract: Thin film solar cells consisting of a glass/ITO/CVD-CdS/CSS-CdTe/ Cu:C/Ag layer system with conversion efficiencies up to 14.4% and (5–8) µm thick CdTe layers as well as CdS(90 nm)/CdTe(6 µm) layers deposited on Si have been investigated by cathodoluminescence (CL) spectroscopy at 5 K. The spectral position of the CdTe exciton line was used to probe the interface region between the n-type CdS layer and CdTe grains at a cleaved edge of the solar cell and neighboring grains at the top of uncovered CdTe layers. For substrate temperatures (T_{sub}) smaller than 610 ^{o}C during the CdTe deposition, the width of the intermixed region between the CdS layer and CdTe grains was found to be smaller than the lateral resolution of the CL ($\approx$300 nm). For T_{sub} as large as (630−650) ^{o}C, a decrease of the CdTe band gap appears to be present up to 0.6 µm from the CdS/CdTe interface. For the grain boundaries, however, a remarkable red shift of the exciton CL line is observed throughout the whole CdTe layer. A $CdCl_2$ treatment homogenizes the distribution of acceptor-like defects or impurities leading to an optimized p-conversion of the CdTe layer.

CL spectra of the CdS window layer exhibit two broad bands centered at 1.72 (red) and 2.04 eV (yellow). Other authors found similar bands in CdS microcrystals and in single crystal CdS bombarded with electrons indicating that the yellow band can be assigned to Cd interstitials. In the solar cells, the yellow band is suppressed by the $CdCl_2$ treatment indicating a passivation or out-diffusion of Cd interstitials.

1. Introduction

One of the promising material systems for solar cell mass production is the p-CdTe/n-CdS/TCO/glass structure. Substantial advance regarding the enhancement of the conversion efficiency was linked to the application of a post deposition $CdCl_2$ treatment of the CdTe layers leading to efficiencies as high as 15.8% at the beginning of the 90th [1]. Since that time no remarkable improvements towards the predicted possible efficiency of about 29% [2] could be achieved. Thus, a more detailed physical understanding of the correlation between material treatment and device performance seems to be essential for further progress. In reference [3], the current state of CdS/CdTe solar cell development is reviewed and 4 key areas are stressed in which advance is urgently demanded. These are related to the CdTe doping in connection with $CdCl_2$ processing, to interface and grain boundary effects, to the development of stable contacts with low barrier, and to the question how different processing steps influence one-another. The challenge for solving problems like these is enlarged by the polycrystalline nature of the layers implicating variations of physical and chemical parameters in both lateral and vertical direction. Since grain sizes of the CdTe layer are usually on the order of micrometers, probes, e.g., for luminescence experiments, with sub-micrometer resolution are desirable.

Spatially resolved methods of investigating the performance and properties of thin film CdS/CdTe solar cells have been reviewed very recently by Edwards et al. [4]. Results of optical and electron beam induced current (OBIC and EBIC) investigations are discussed in detail. The $CdCl_2$ treatment was found to cause a homogenization of the EBIC response and a passivation of the grain boundaries. Moreover, an enhancement of the apparent p-doping near to the grain boundaries was established. A few cathodoluminescence (CL) investigations of bevelled CdTe layers led to the conclusion that the distribution of native defects and impurities between grains in the cell is complex. The obtained CL spectra were obviously averaged over several grains. Therefore, different bound excitons could not be resolved.

In this work, comprehensive CL investigations of the CdTe and CdS layers in solar cell structures are discussed. The spectral peak position of distinct bound excitons is used to probe the lateral doping distribution and the intermixed layer at the CdS/CdTe interface as a function of the $CdCl_2$ treatment and CdTe deposition temperature. Moreover, we obtained new information about the variation of electronic properties in the CdS window layer as a result of the post-growth $CdCl_2$ treatment.

2. Experimental

CdTe thin film solar cells with a glass/ITO/CVD-CdS/CSS-CdTe/Cu-doped carbon/Ag structure were fabricated under different growth and post-growth $CdCl_2$ treatment conditions. The $6 - 8$-µm-thick CdTe layers were deposited on a glass (Corning 1737) substrate with a 250-nm-thick ITO film and a $60 - 80$-nm-thick CdS layer. In order to enable investigations of the free CdTe surface and to relieve the cleavage of such structures CdS (90 nm)/CdTe(6 µm) layer structures were deposited under comparable conditions on Si substrates. More details about the fabrication procedure can be found elsewhere [5]. Table I contains the most essential parameters of the investigated samples along with the resulting conversion efficiencies of the completed devices.

Table I: Substrate temperature during the CdTe deposition (T_G), temperature of the $CdCl_2$ treatment (T_{CdCl2}), and conversion efficiency (Eff.) of the solar cell devices and Si/CdS/CdTe structures under investigation

glass/ITO/CdS/CdTe/C/Ag structures					Si/CdS/CdTe structures		
sample	**T_G (^{o}C)**	**T_{CdCl2} (^{o}C)**	**Eff. (%)**		**sample**	**T_G (^{o}C)**	**T_{CdCl2} (^{o}C)**
#118	595	without	5.8		#759	600	without
#136	595	460	7.1		#766	600	460
#290	610	415	13.7		#764	600	415
#260	630	415	14.1				
#265	650	415	12.7				

As observed by many authors, most important for the achievement of a high conversion efficiency is a proper choice of the $CdCl_2$ treatment conditions. For this, we found an optimum at 415°C. Moreover, a suitable temperature regime during the CdTe deposition is also necessary which has been discussed more in detail elsewhere [6]. For the examples of Table I, an increase of the substrate temperature exceeding 630°C leads to a decrease of the efficiency. Consequently, the investigations to be discussed below were related to the effect of both the $CdCl_2$ treatment and of the deposition temperature on the spatial and spectral cathodoluminescence distribution in selected samples.

CL spectra, line profiles, and images were obtained in a scanning electron microscope (SEM) equipped with an Oxford mono-CL2 and He-cooling stage system allowing for temperatures down to 5 K. A grating monochromator and a cooled photomultiplier as well as a CCD photodetector were used to disperse and detect the CL signal. The electron beam energy was chosen to be 5 keV and the current amounted to $0.1-1$ nA. The sample temperature amounted generally to 5 K.

3. Results and Discussion

3.1. Inspection of the CdTe surface

In the first part of the discussion, we focus on the influence of the $CdCl_2$ treatment on the lateral distribution of distinct excitonic lines. Thus, CL data obtained from the top of the CdTe layers grown on the Si/CdS substrate (right hand side of Table I) will be considered in the following. Figures 1 and 2 show secondary electron (SE) images and CL spectra of as-grown and $CdCl_2$ treated layers, respectively. Most of the grains of the polycrystalline CdTe layers are twined and the diameter of the largest ones is comparable with the layer thickness ($\approx 5 - 6$ µm). For an excitation area corresponding to the depicted SE images, CL spectra (not shown) exhibit a broad near band edge line where different excitonic contributions can hardly be distinguished. Reasons for this are the high defect density and the inhomogeneous distribution of defects and impurities in these systems [4,7]. As demonstrated in Figs. 1 and 2, distinct exciton transitions can actually be resolved if the excitation is restricted to single CdTe grains. The depicted CL spectra were recorded for a number of spot excitations along a certain path (cf., short dotted lines marked in the SE images). The left hand side of the respective paths corresponds to the scan position zero. In both sets of CL spectra, we observe exciton lines at 1.588, 1.590 (acceptor-bound excitons [8]), and at $1.592-1.594$ eV (donor bound exciton [9,10]). For the as-grown sample, an additional line is observed at about 1.596 eV (free exciton with n=1 [9]). Consequently, the exciton spectra excited by the focussed electron beam can be used to probe the distribution of impurities and/or defects acting as acceptors or donors between neighboring grains or even within a single grain.
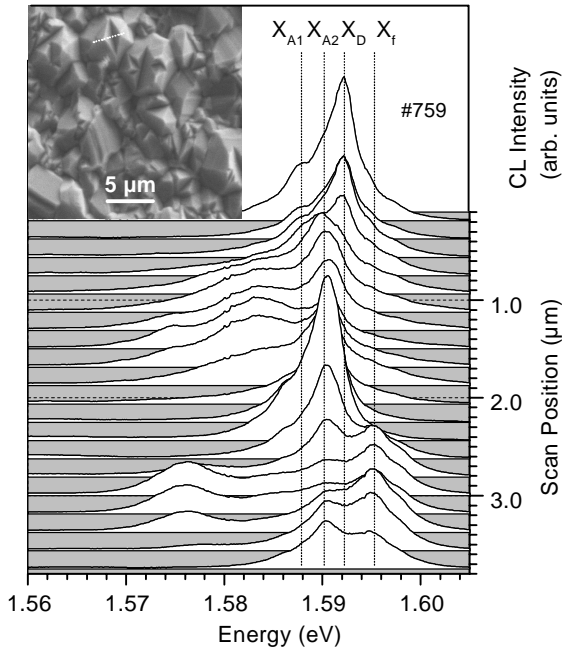
Fig. 1. SEM image and CL spectra of an as-grown CdS/CdTe structure on Si. The CL spectra were excited at various spots along a path corresponding to the marked dotted line in the SEM image. The left hand side of the path is equal to the scan position zero.
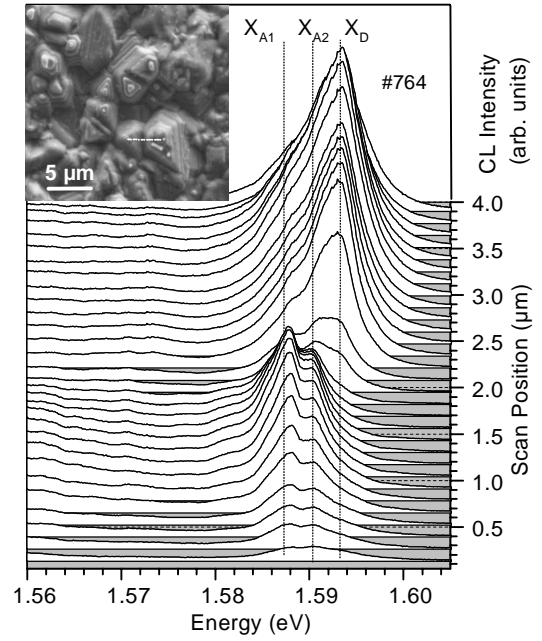

Fig. 2. SEM image and CL spectra of a $CdCl_2$ treated CdS/CdTe structure on Si. The CL spectra were excited at various spots along a path corresponding to the marked dotted line in the SEM image. The left hand side of the path is equal to the scan position zero.

With regard to this important question, we establish that defects or impurities are obviously rather inhomogeneously distributed in both the as-grown and $CdCl_2$ treated sample. However, while the doping seems to vary randomly within a single grain of the as-grown sample, it mainly varies between grains in the $CdCl_2$ treated one. As can clearly be seen in Fig. 2, in the small grain (left hand side), all the CL spectra are dominated by acceptor bound excitons (X_{A1}, X_{A2}), whereas in the large grain (right hand side), all the CL spectra are dominated by the donor bound exciton (X_D). The CL spectra in Fig. 2 reflect a general trend observed for many grains in $CdCl_2$ treated samples: small grains and the periphery of large grains are dominated by p-type doping, whereas the centers of large grains are dominated by n-type doping. The effect of the $CdCl_2$ treatment on the general doping distribution becomes more clearly visible in the CL images of Fig. 3. In Fig. 3(b) and (e), the CL detection energy was set to the peak position of the donor bound exciton and in (c) and (f) to 1.585 eV (low energy side of the acceptor bound excitons). While for both without and with $CdCl_2$ treatment the donor bound exciton is essentially restricted to the center of large grains, CL from acceptor bound excitons is detected for almost each grain of the excited area and from the periphery of large grains only after $CdCl_2$ treatment [11].

Fig. 3. Secondary electron (a, d) and CL (b, c, e, f) images of CdTe layers. For (b) and (e) the CL detection energy was set to 1.592 eV and for (c) and (f) it was set to 1.585 eV,

This result confirms observations of Edwards et al. [4], who found a more uniform electron beam induced current responds and a higher p-carrier concentration near to the grain boundaries after the $CdCl_2$
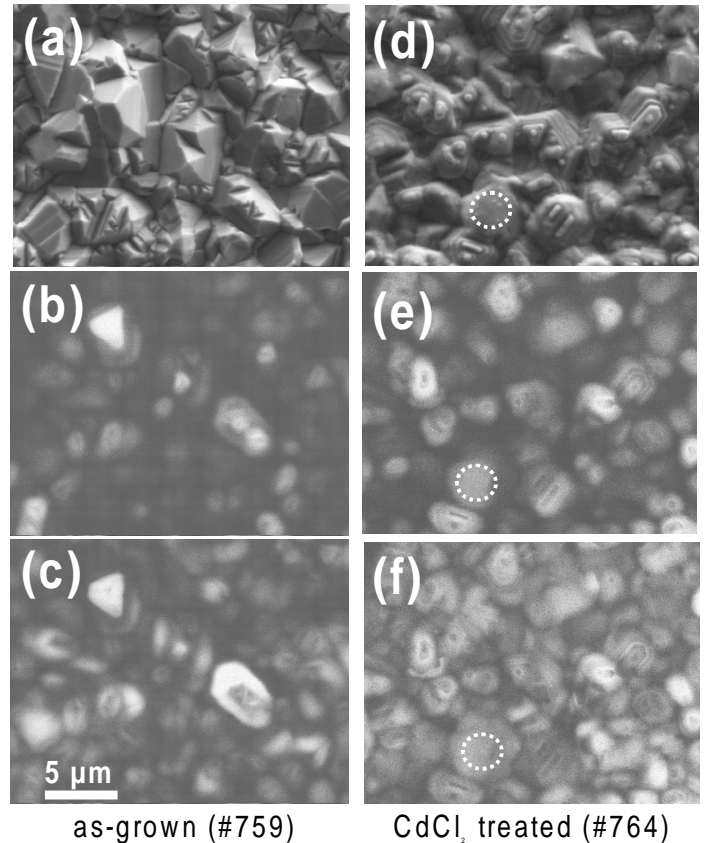
treatment of CdS/CdTe solar cells. Moreover, it provides a graphic impression of the conversion of poly-crystalline CdTe to a closed p-type layer as a result of the $CdCl_2$ treatment, which has been generally established by various authors (see, e.g., reference [3]). A heat treatment related p-conversion was proven to be caused by the generation of Cd vacancies acting as acceptors in CdTe [12,13]. Moreover from a theoretical point of view, the presence of chlorine is predicted to further promote p-type doping of CdTe by the formation of a Cd vacancy-chlorine complex which ionization energy is expected to be 30 meV below that of the Cd vacancy [14]. Therefore, we assume that a chlorine diffusion into small grains and within a border region of large grains during the $CdCl_2$ treatment promotes remarkably the p-type conversion of the CdTe layers.
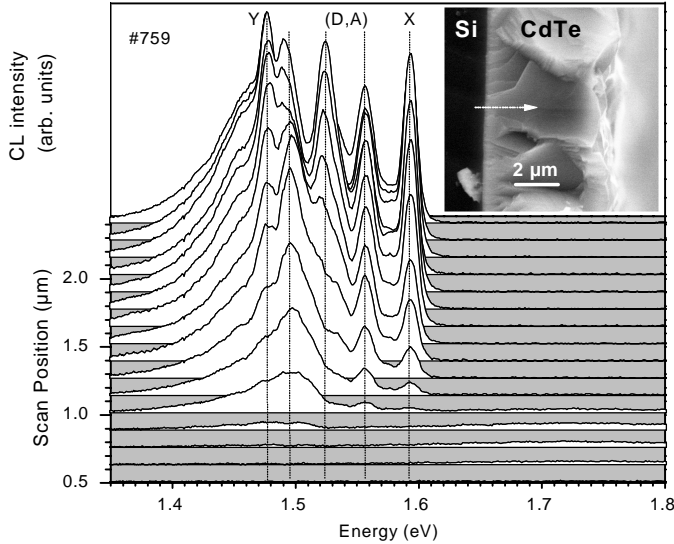

Fig. 4. Secondary electron (SE) image and CL spectra of the cleaved edge of an as-grown CdS/CdTe structure deposited on Si. The spectra were excited at various spots along the path marked by the dotted line in the SEM image.
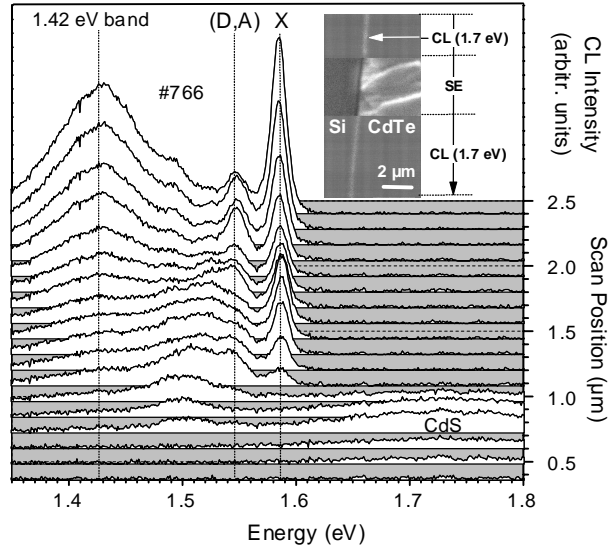
Fig. 5. Combined SE/CL image and CL spectra of the cleaved edge of an $CdCl_2$ treated CdS/CdTe structure deposited on Si. The spectra were excited at various spots along a path perpendicular to the layers crossing the CdS/CdTe interface. Scan position zero corresponds to the starting point at the Si substrate

3.2. Inspection of the CdS/CdTe interface region at the cleaved edge

The second part of the discussion refers to the influence of a $CdCl_2$ treatment and of the deposition temperature on the exciton energy within the near-interface regions of CdTe grains. Respective CL investigations were performed at the cleaved edge of CdTe layers deposited on Si/CdS substrates and of completed solar cell devices on glass/ITO/CdS substrates (see Table I). As in the case of the surface inspection, we performed the CL measurements at unpolished edges to prevent the influence of polish related defects or changes of strain on the electronic properties of the material. Fig. 4 depicts a SE image of a cleaved Si/CdS/CdTe layer structure. In order to probe the properties of the n-CdS/p-CdTe interface, CL spectra are acquired along a line perpendicular to the layers crossing the Si/CdS/CdTe region (cf., dotted line in the inset). For investigations like this, smoothly cleaved, large grains have been chosen. Thus, the following consideration refers to features of CdTe grains and their interface with respect to the CdS layer essentially excluding grain boundary effects.

Figures 4 and 5 show respective sets of CL spectra of an as-grown and $CdCl_2$ treated Si/CdS/CdTe system, respectively. Each scan starts at the substrate (scan position zero) and ends in the CdTe layer. Approaching the CdS/CdTe interface, the electron beam excitation firstly generates a broad CL spectrum within an energy range far above the CdTe band gap (for E > 1.6 eV). This CL signal appears independently on the respective substrate (Si/CdS, or glass/ITO/CdS) if the electron beam just passes the very close interface region. The inset of Fig. 5 shows a combined CL/SE image of the cleaved edge of a Si/CdS/CdTe structure. While the electron beam was scanning downwards, the signal has been switched between the CL (detection energy: 1.7 eV) and SE signal. The comparison of the three parts of the image clearly confirms that the CL signal at 1.7 eV arises exclusively within the interface region between substrate and CdTe layer, thus, suggesting that this part of the spectrum originates from the thin CdS window layer. Its nature is

briefly discussed below. For the moment, we solely stress the importance of the CdS related CL as a marker of the CdS/CdTe interface position with regard to the scan position of the electron beam.

Immediately after passing the CdS layer, the usually observed lines of the CdTe spectrum near its band gap [bound exciton at about 1.59 eV and (D,A)-pair transitions at about 1.55 eV] appear in both samples without any notable spectral shift. The exciton CL lines are strongly quenched near the interface which is probably caused by interface states and/or by the electrical field within the depletion layer of the p-n junction. Far away from the interface, the spectra of the samples without and with $CdCl_2$ treatment show − as usually observed − different spectral features in the low-energy range (see, e.g., Okamoto et al. [5]). While the as-grown sample gives rise to further distinct lines which are connected with different (D,A)-pairs and the so-called Y luminescence at 1.477 eV, the grain of the $CdCl_2$ treated sample is characterized by a broad band centered at about 1.42 eV. Decreasing the distance with respect to the interface causes a rapid decrease of the CL lines at 1.52 eV and 1.475 eV for the as-grown sample as well as of the (D, A)-pair line and 1.42 eV band for the $CdCl_2$ treated one leaving in both cases a broad CL band centered at about 1.5 eV for the interface region. These "near-interface-spectra" resemble closely the PL spectra obtained by junction excitation [5] which are − consistently with our CL observations − not remarkably different in as-grown CdS/CdTe layer structures compared with $CdCl_2$ treated ones.

Figure 6 summarizes the data of Fig. 4 and provides an experimental estimate of the lateral resolution of the electron beam probe under the used conditions (T = 5 K, electron beam energy = 5 keV). The circles and full squares are the integrated intensities of the CdS related and CdTe exciton CL, respectively. The stars indicate the spectral position of the exciton line as a function of the scan position with regard to the CdS layer (scan position zero). Since the thickness of the CdS layer (90 nm) is smaller than the expected diameter of the excitation volume, the profile of this layer cannot be resolved. Instead, we obtain a Gaussian shaped profile with an FWHM of 365 nm, indicating a lateral resolution of the CL mode of about 300 nm. This value is in accordance with an estimated diameter of the electron scattering volume of about 200 nm and a minority carrier diffusion length, which is expected to be remarkably smaller than 300 nm at 5 K [4].

Within this spatial resolution, a decrease of the exciton peak position − thus, a reduction of the CdTe band width due to intermixing at the CdS/CdTe interface − could not be observed in the as-grown sample even for the closest distance of about 100 nm from the center of the CdS layer.

In Fig. 7(a), scans like this are compared for samples experienced different growth and $CdCl_2$ treatment temperatures. As can be clearly seen, the described situation does not change remarkably with $CdCl_2$ treatment even for temperatures up to 460°C. The jump of the exciton energy of sample #764 (stars) from 1.5965 eV down to 1.590 eV near the interface is rather due to inhomogeneous doping within the respective grain (coexistence of regions

Fig. 6. Integrated intensity of the CdS related CL (circles) and of the CdTe exciton line (squares) as well as the spectral position of the CdTe exciton line (stars) as a function of the scan position of the electron beam with regard to the center of the CdS layer. The data correspond to Fig. 4.

dominated by free excitons with those dominated by acceptor bound ones) than to an abrupt narrowing of the band gap. An increase of the growth temperature, however, led to a notable gradual red-shift of the exciton energy down to values, for which bound exciton levels are not expected in CdTe. This increasing red-shift with decreasing distance to the interface is obviously due to an intermixed layer, which thickness increases remarkably if T_G becomes larger than 600°C. Furthermore, at the highest deposition temperature an overall lowering of the exciton energy down to 1.585 eV was observed. This excitonic energy level has been assigned to a deep acceptor bound exciton associated with Cd vacancies [9]. Consequently, CdTe deposition
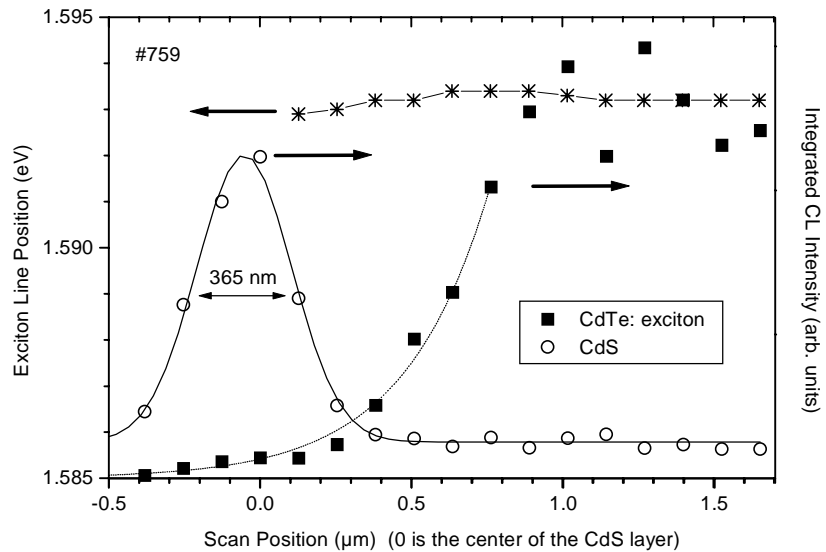
at substrate temperatures larger than 600°C promotes both the formation of a rather thick intermixed layer and the generation of Cd vacancies. Note again, that the discussed results refer rather to the CdTe grains than to grain boundary effects!
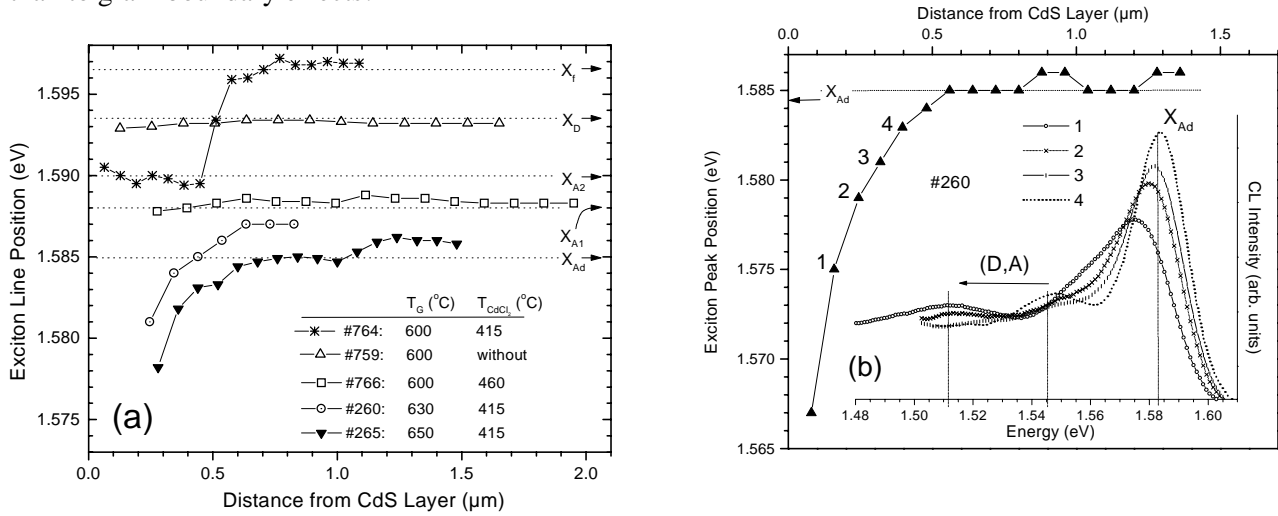

Fig. 7. Spectral peak position of the CdTe exciton line as a function of the distance from the center of the CdS layer for different CdCl$_2$ treatment conditions and substrate temperatures during the CdTe deposition. X_f, X_D, X_{A1}, X_{A2}, and X_{Ad} mark the peak positions of the free, donor bound, acceptor bound (acceptors A1, A2, and deep acceptor), respectively. Inset of (b): CL spectra at the scan positions 1...4.

With regard to the portion of sulfur within the intermixed layer we have to take into account that the CL averages over a layer thickness of about 300 nm. Consequently, the amount of sulfur can not be determined directly from the exciton peak position. Nevertheless, considering the shape of the spectra − instead of only the peak position − the composition range of the interface region can roughly be estimated. The inset of Fig. 7(b) shows four CL spectra of the CdTe layer grown at 630°C (#260) for various distances of the exciting electron beam with respect to the CdS layer. The spectra 1...4 correspond to the exciton peak positions marked by 1...4 in Fig. 7(b). Approaching the CdS/CdTe interface, the red-shift of the exciton peak position is accompanied by a broadening of the spectrum which is more pronounced at the low-energy side. The low-energy tail of the spectrum represents regions with large sulfur portions. The exciton spectrum of position 1 extends down to about 1.55 eV. Taking into consideration a value of the exciton energy in the unmixed CdTe of 1.585 eV (saturation level for large distances), we estimate a narrowing of the band gap of about 35 meV. This value is consistent with the observed shift of the (D,A)-pair band from 1.55 eV (unmixed CdTe) down to 1.515 eV. A reduction of the CdTe band gap energy by 35 meV corresponds to a CdS mole fraction of 0.037 [15]. Similar results were obtained by Grecu and Compaan [16] by junction PL of CdS/CdTe solar cells on commercial glass/SnO$_2$ substrates.

Since alloy formation could not be proved for T_G = 600°C and for higher values of T_G it was observed only for distances from the interface comparable with the lateral resolution, the intermixed layers of CdTe-grains are probably very thin. Indeed, if we take into account the maximum values of the diffusivity of sulfur in single crystal CdTe found by Lane et al. [17], we obtain diffusion length of about 20 and 60 nm for sulfur in CdTe at 600°C (30 s) and 650°C (60 s), respectively [the use T_G (time) values correspond to our deposition conditions]. In consideration of this result we conclude that spatially integrated experiments revealing intermixed layers as thick as several 100 nm or few μm are most probably strongly influenced by fast diffusion of sulfur within grain boundaries and extended defects [3,7].

In Fig. 8, the peak energy of the CdTe exciton line is depicted as a function of the scan position along a line not perpendicular to the interface but parallel to the layers 1.5 μm apart of the CdS/CdTe interface. Again, the general exciton level depends on the value of the growth temperature. While for T_G = 610 °C (#290), the peak energy varies between the donor and acceptor bound excitons, it fluctuates around 1.585 eV for higher value of T_G. However, at a certain position of sample #260, we establish an unexpected reduction of the exciton energy down to about 1.580 eV. We assign such drops of the exciton energy which could be established even in the middle range of the CdTe cross-section to grain boundaries or extended defects giving rise to fast sulfur diffusion and, therefore, to a lowering of the CdTe band gap at certain regions even far away from the CdS/CdTe interface.
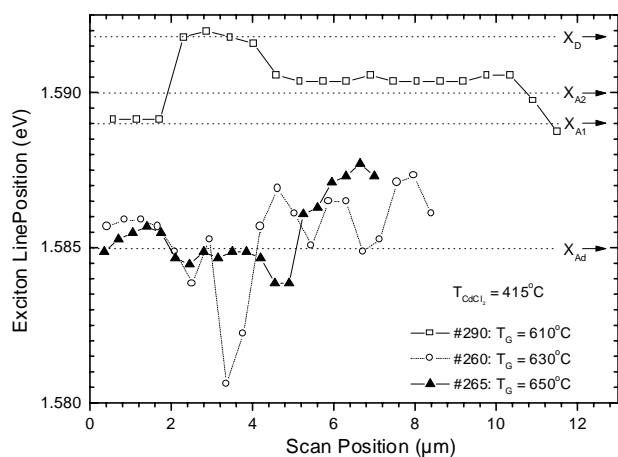
Fig. 8. Spectral peak position of the CdTe exciton CL line excited at various spots along a path on the cleaved edge parallel to the layer 1.5 µm apart of the CdS/CdTe interface. The curves differ in the substrate temperature during the CdTe deposition.
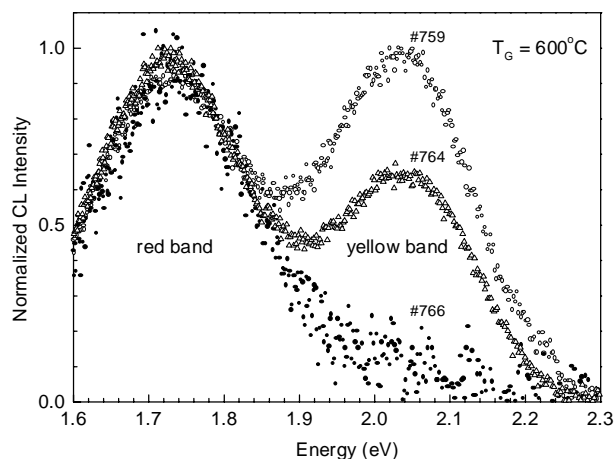
Fig. 9. CL spectra of the CdS window layer excited at the cleaved edge of a CdS(90 nm)/CdTe(6 µm) structure for different $CdCl_2$ treatment conditions.

3.3. The CdS window layer

For excitation within the interface region, we obtained a CL signal at photon energies far above the CdTe band gap which can be assigned to the thin CdS window layer (cf. Figs. 4 and 5). The whole spectral range for which we observe this luminescence is depicted in Fig. 9. Three spectra are shown differing in the $CdCl_2$ treatment conditions. They consist of a broad red band and an even broader yellow one centered at 1.72 and 2.04 eV, respectively. The intensities are normalized to the respective peak intensity of the red band. At this point it is interesting to note that Agata et al. [18], who investigated luminescence properties of gas-evaporated CdS, found also a red and a yellow PL band in micro-crystals 72 nm in average size. The authors assign the red band to transitions of electrons trapped at surface states to the valence band and the yellow one to a deep donor to valence band transition with Cd interstitials as the donors. Kulp [19] performed electron bombardment experiments at single crystal CdS and identified the luminescence bands at 1.72 and 2.04 eV to be due to the sulfur vacancy and Cd interstitial, respectively. Thus the yellow band can be undoubtedly assigned to the Cd interstitial. The CL intensity of this CL band is remarkably reduced and almost completely disappeared after $CdCl_2$ treatment at 415°C and 460°C, respectively. Since after the $CdCl_2$ treatment a considerable chlorine accumulation at the interface has been observed by several authors (see, e.g., [7,20]) an effect of such a treatment on the CdS layer can be strongly expected. Therefore, it is suggested that Cd interstitials are passivated or their out-diffusion is promoted by the $CdCl_2$ treatment.

To what extent the $CdCl_2$ related quenching of the yellow CL band in the CdS spectrum is linked to the abrupt decrease of the conversion efficiency for treatment temperatures as high as 460°C is not yet clear and further experiments are necessary for a better understanding.

References

[1] J. Britt, C. Ferekides, Appl. Phys. Lett. **62**, 2851 (1993).

[2] De Vos, J.E. Parrot, P. Baruch, P.T. Landsberg, Proceedings of the 14th European Photovoltaic Solar Cell Energy Conf., Amsterdam, 1315 (1994).

[3] K. Durose, P.R. Edwards, D.P. Halliday, J. Crystal Growth **197**, 733 (1999).

[4] P.R. Edwards, S.A. Galloway, K. Durose, Thin Solid Films **361-362**, 364 (2000).

[5] T. Okamoto, Y. Matsuzaki, N. Amin, A. Yamada, and M. Konagai, Jpn. J. Appl. Phys. **37**, 3934 (1998).

[6] T. Okamoto, Y. Harada, A. Yamada and M. Konagai, to be published in: Proc. 11th Int. Photovoltaic Science and Engineering Conf., Hokkaido, Japan, 1999, Sol. Energy Mat. & Sol. Cells, Special Issue.

[7] R. Dhere, D. Rose, D. Albin, S. Asher, M. Al-Jassim, H. Cheong, A. Swartzlander, M. Moutinho, T. Coutts, R. Ribelin, and P. Sheldon, Proccedings of the 26th International Conference on Photovoltaic Solar Cells, 1997, Anaheim, pp. 435.

[8] E. Molva, J. L. Pautrat, K. Saminadayar, G. Milchberg, and N. Magnea, Phys. Rev. B **30**, 3344 (1984).

[9] K.A. Dhese, D.E. Ashenford, J.E. Nicholls, P. Devine, B. Lunn, C.G. Scott, and J. Jaroszynski, J. Crystal Growth **138**, 443 (1994).

[10] J.S. Gold, T.H. Myers, N.C. Giles, K.A. Harris, L.M. Mohnkern, and R.W. Yanka, J. Appl. Phys. **74**, 6866 (1993).

[11] Among others, the detailed CL intensity fluctuation is influenced by the surface morphology. Thus, statements about concentration variations of acceptors are not possible.

[12] B.M. Basol, S.S. Ou, and O.M. Stafsudd, J. Appl. Phys. **58**, 3809 (1985).

[13] J.M. Figueroa, F. Sanchez-Sinencio, J.G. Mendoza-Alvarez, O. Zelaya, C. Vazquez-Lopez, and J.S. Helman, J. Appl. Phys. **60**, 452 (1986).

[14] Su-Huai Wei and S.B. Zhang, to be published in: Proceedings of the 28th IEEE Photovoltaic Specialists Conference, Anchorage, AK, USA, September 15-22, 2000.

[15] K. Ohata, J. Saraie, and T. Tanaka, Jpn. J. Appl. Phys. **12**, 1641 (1973).

[16] D. Grecu and A.D. Compaan, Appl. Phys. Lett. **75,** 361 (1999).

[17] D.W. Lane, G.J. Conibeer, D.A. Wood, K.D. Rogers, P. Capper, S. Romani, and S. Hearne, J. Crystal Growth **197**, 743 (1999).

[18] M. Agata, H. Kurase, S. Hayashi, and K. Yamamoto, Solid State Commun. **76**, 1061 (1990).

[19] B.A. Kulp, Phys. Rev. **125**, 1865 (1962).

[20] K. D. Dobson, I. Visoly-Fisher, G. Hodes and D. Cahen, Solar Energy Materials & Solar Cells **62,** 295 (2000).